PHYSICAL REVIEW B VOLUME 25, NUMBER 12 15 JUNE 1982

Electron-gas model for molecular crystals. Application to the alkali and alkaline-earth hydroxides

R. LeSar* and R. G. Gordon
Department of Chemistry, Harvard University, Cambridge, Massachusetts 02138
(Received 8 January 1982)

A theoretical model for calculating the structure and energy of molecular crystals is presented. The model, which requires no empirical parameters, is based on the Gordon-Kim electron-gas model. Many-body effects are incorporated through the mutual overlap of the electronic distributions of all molecules or ions in the neighborhood of a given point in the crystal. Effects of the crystal environment on the molecular properties are approximated by inclusion of an electrostatic potential that mimics the crystal potential in *ab initio* calculations on the individual component molecules or ions in the crystal. Application is made to a number of alkali and alkaline-earth hydroxide crystals in which the components are taken to be hydroxide ions, and alkali or alkaline-earth cations. The agreement with experiment is good (within 2.5% in lattice constants and 1.1% in lattice dissociation energy). The calculated changes in molecular dipole moment are between 20 and 40%.

I. INTRODUCTION

A number of theoretical methods have been developed to calculate the properties of molecular crystals. Optimally, such a theory should satisfy three conditions: The theory should describe well the anisotropies of the intermolecular interactions (dynamical properties in particular depend critically on the shape of the energy surface), it should be usable in a predictive sense where experimental results are not available, and the calculations should not be prohibitively expensive. As of now, no method has entirely satisfied these three conditions.

The most commonly used method used to calculate properties of molecular crystals has been to express the total interaction energy as a sum over the pair interactions between the molecules in the crystal.[1] The difficulties with this method arise in determining accurate forms for the short-range repulsive forces between the molecules. One of the primary difficulties in finding an expression for these repulsions between molecules is that the potentials are often highly anisotropic. In particular, it is not easy to extract good information about the anisotropy of the pair potentials from experimental data. Fitting the parameters in the short-range potential to pressure-volume data in solids, an approach often taken to find pair potentials,[2] is ambiguous, since in a crystal the nearest neighbors are in just a few sets of relative orientations and only limited regions of the pair potentials are sampled. The potentials found to fit these experimental data are really only appropriate for the positions and orientations in the experimental system and thus cannot be used with any confidence to describe either other forms of the crystal, or a general orientation of the molecules. In principle, obtaining information about the pair potentials from data on lattice vibrations offer a better sampling of the pair potentials because the vibrational frequencies depend on a larger portion of the potential surface.[3] However, the complexities of the pair potentials make it difficult to find an unambiguous representation of the potential from this data. Molecular-beam scattering has been used primarily to obtain the isotropic part of the potential, except for such relatively simple systems as the H_2—inert-gas potentials.[4] One can also obtain some information about anisotropic potentials from the second virial coefficient, but again the data do not uniquely determine the short-range potential.[5] The best experimental approach has been to find the intermolecular pair potentials that show best agreement with all available data.

Traditional theoretical methods of calculating the short-range pair potentials, such as the Hartree-Fock self-consistent-field method (SCF), are time consuming and subject to errors which are

difficult to estimate.[6] For molecular interactions in particular, where the potential between the molecules is a function of many variables, to get a good representation of the potential, many points on the potential surface are needed. Because of the difficulty and expense of obtaining a high-quality calculation of the pair potential with these methods, relatively few molecular crystals have been studied using theoretically determined potentials.[7]

Recently, Gordon and Kim have developed a relatively simple *a priori* method of calculating the short-range interactions between molecules, the electron-gas model (GK).[8,9] In its original formalism, and in a later version (the modified electron-gas model, MEG),[10] this model has been shown to give pair potentials that are in good agreement with experimentally determined potentials. The total short-range energy is written as a sum of contributions representing the exchange, kinetic, correlation, and nonpoint Coulomb interactions. Each of these terms can be expressed as a simple functional of the electronic density, which is taken to be a superposition of densities calculated from Hartree-Fock wave functions found for the isolated molecules. The main advantages to this method over traditional *ab initio* methods are that it takes much less computer time for each potential point and that the time for each calculation is essentially independent of the size of the molecules involved.

The electron-gas model has been applied quite successfully to the calculation of properties of ionic crystals containing monatomic ions. In the work by Kim and Gordon[11] and Cohen and Gordon,[12] the binding energy of a crystal was expressed as a sum of point Coulomb (Madelung) energies and a short-range energy which was calculated as a sum of pair potentials calculated with the GK model in the Kim and Gordon calculations and the MEG model in the Cohen and Gordon case. Recently, an electron-gas theory for ionic crystals that includes many-body effects has been developed by Muhlhausen and Gordon.[13] This model has given very good agreement with experiment for a wide variety of ionic crystals. Boyer has used potentials generated by the electron-gas model to study the lattice vibrations of some ionic salts, with particular attention to the solid-liquid transition.[14]

While the use of the electron-gas model greatly simplifies the calculation of intermolecular potentials, the complexity of these potential surfaces makes it prohibitively time consuming to find all potentials needed for all crystals of interest. Methods where the energy of the crystal is determined directly, and not as a sum of pair potentials, should provide more efficient calculational schemes. *Ab initio* methods based on Hartree-Fock theory have been developed to calculate the energies of crystals without using the pair potential formalism.[15] These calculations are mathematically and numerically difficult, and the approximations necessary to overcome these problems make these theories either inaccurate or impractical for calculations on most crystals.

Here we present a theoretical model for molecular crystals, similar to the many-body electron-gas model for atomic ionic crystals of Muhlhausen and Gordon,[13] that eliminates the need for calculating the intermolecular pair potentials and requires no empirical parameters. The binding energy calculated with this method includes two types of many-body effects. One type is due to distortions of the electronic density of a molecule in the crystal due to the fields produced by all other molecules in the crystal. The second type is due to the nonlinearity of the electron-gas functionals and represents the short-range energy due to the mutual overlap of more than two charge distributions. Although the model is used here for crystals containing only linear molecules, the method is general and could be extended to crystals containing more complicated molecular units. A simplification of the present model is that the molecular electronic densities are represented as sums of spherically symmetric functions. Thus, only small modifications to the equations derived by Muhlhausen and Gordon[13] for monatomic ionic crystals are necessary for the molecular case.

One of the approximations in the original electron-gas model is to take as the electron density a superposition of densities calculated from gas-phase Hartree-Fock wave functions, which is appropriate in regimes where there is no significant distortion of the density. In ionic crystals, where there are large electrostatic potentials due to the charges in the system, the electronic density of the molecular ions can have large anisotropic distortions. We treat these distortions by including a term in the Hamiltonian which approximates the effects of the potentials, and by determining the molecular wave function by Hartree-Fock methods as usually applied to small molecules. We discuss below how these distortions in the electronic density can change such molecular parameters as the dipole moment. The method used here for molecules

is similar to that used for spherical ions in the Muhlhausen-Gordon theory and by others.[16,17]

In Sec. II the appropriate equations for the calculation of the crystal energies are presented. Included in this section are: a review of the modified electron-gas theory, a discussion of the method of representing the molecular densities, and a derivation of the model. In Sec. III we describe the numerical methods used here in calculating the crystal energy. Section IV is devoted to a discussion of the model used here for incorporating the distortions in the electronic charge distributions due to the crystal fields. Also included in Sec. IV is a discussion of the thermodynamic cycles appropriate for this model. Application of the model to alkali and alkaline-earth hydroxides is made in Sec. V.

II. THEORY

In this section we present the appropriate equations for the calculation of the binding energy of a molecular crystal. We restrict the discussion to crystals involving linear molecules, and in particular to ionic crystals, where dispersion energies make small contributions to the binding energy.

The model used here is similar to that of the Muhlhausen-Gordon model for simple ionic crystals.[13] Like Muhlhausen and Gordon, we divide the binding energy W_B into four components

$$W_B=(W_E+W_K+W_X+W_C)/n \ , \tag{1}$$

where W_X, W_K, and W_C are the exchange, kinetic, and correlation energies calculated from the MEG theory. The total electrostatic energy W_E consists of a point Coulomb (Madelung) term and a term corresponding to the electrostatic energy due to the overlap of two charge distributions. Since the energy as calculated here is the energy of a unit cell, the binding energy is obtained by dividing the total energy by n, the number of formula units per unit cell.

A. The modified electron-gas theory

In the GK model, the interaction energy between closed-shell systems is evaluated as a functional of the electronic density of the systems. The total electron density is approximated by a sum of densities of the interacting systems, where the component densities are taken from Hartree-Fock calculations on the individual systems. In a two-body system, the total density is $\rho_{AB}=\rho_A+\rho_B$, where ρ_A and ρ_B are the component densities. The energy is a sum of terms corresponding to the kinetic, exchange, correlation, and electrostatic energies of the system.

The electrostatic energy between two systems can be readily evaluated in terms of the electron densities and the nuclear charges. The electron-gas terms are of the form

$$W_i=\int d\vec{r}\{\rho_{AB}(\vec{r})E_i[\rho_{AB}]-\rho_A(\vec{r})E_i[\rho_A] -\rho_B(\vec{r})E_i[\rho_B]\} \ , \tag{2}$$

where the density functionals E_i are for the exchange, kinetic, and correlation energies, respectively.[8] The integrations in Eq. (2) are carried out numerically.

The functionals presented here were derived for a uniform electron gas, while in a system of interacting molecules the electronic density is clearly not uniform. In an attempt to correct the functionals to deal with this nonuniformity, Waldman and Gordon have introduced scale factors for the functionals (the modified electron-gas model, MEG).[10] These scale factors are uniquely determined for an interacting system by requiring the energy functional to give correct results for the corresponding energy term for the atom isoelectronic to the system.

B. Representation of molecular densities

For the calculation of the MEG pair potentials the electron densities of the interacting systems are needed. For atomic systems, where the densities are spherically symmetric, the density can be calculated from a Hartree-Fock wave function as a function of distance and can then be represented by a one-dimensional interpolation. For molecules the problem is not quite so straightforward. For linear molecules a two-dimensional interpolation scheme could be used, as is done in other electron-gas programs.[18,19] A large number of points is needed, however, to get a good representation of the density. For this reason, and for simplification of the numerical calculations, we have chosen to represent the molecular electronic densities as a sum of spherically symmetric functions centered at various points along the bond.

Recently, Parker, Snow, and Pack presented a program for the calculation of linear molecule-linear molecule pair potentials, using the electron-gas model, where they found it useful to expand

the density (calculated from Hartree-Fock theory) of at least one of the molecules in a basis of Slater functions.[19,20] We have taken the same type of approach here. For a linear molecule with m nuclei the density $\rho(\vec{r})$ is expanded as a sum of n spherically symmetric functions ($n \geq m$) located along the axis at $\vec{r}_i$,

$$\rho(\vec{r}) \approx \rho'(\vec{r}) = \sum_{i=1}^{n} \rho_i(|\vec{r}-\vec{r}_i|) , \tag{3a}$$

where

$$\rho_i(r) = \sum_{p=1}^{N} a_{ip} r^{n_{ip}-1} e^{(-Z_{ip}r)} . \tag{3b}$$

The coefficients $\{a_{ip}\}$ are determined by a linear least-squares minimization of $(1-\rho'/\rho)^2$, where a modified version of the Parker-Snow-Pack program is used.[19] By choosing the appropriate functions and number of centers, fits with a relative standard deviation of less than 1% were possible for most systems.

For a molecular crystal, the total density is written as a superposition of densities due to the individual molecules and takes the form

$$\rho_E(\vec{r}) = \sum_i \sum_{j=1}^{n_i} \sum_{\vec{l}} \rho_{ij}(\vec{r}-\vec{r}_{ijl}) , \tag{4}$$

where here and below the sum over i is a sum over the molecules in the unit cell, the sum over j is a sum over the centers in molecule i and the sum over $\vec{l}$ is a sum over the lattice vectors. The vector,

$$\vec{r}_{ijl} = \vec{r}_j + \vec{r}_i + \vec{r}_l ,$$

locates the jth center of the ith molecule in the unit cell denoted by $\vec{r}_l$. The molecular densities used here are determined from Hartree-Fock wave functions found in calculations on the individual molecules. The methods used to approximate the effects of the crystal environment on the charge distributions will be described below. The spherically symmetric densities ρ_{ij} are tabulated at the beginning of each calculation and found when needed by a cubic-spline interpolation.

C. Molecular crystal energies

1. Electron-gas terms

The electron-gas interaction energy per unit cell for the kth component can be written as

$$W_k = \int_V d\vec{r}\, E_k[\rho_E(\vec{r})] - \sum_i \int d\vec{r}\, E_k\left[\sum_{j=1}^{n_i} \rho_{ij}(\vec{r}-\vec{r}_{ij})\right] ,$$

where the sum over j is a sum over the centers in molecule i. The integral in the first term is over the unit-cell volume V and represents the total energy of the unit cell, while that in the second term is over all space and contains the self-energy terms of the individual molecules. The density ρ_E is given in Eq. (4) and is the total electronic density from all molecules in the crystal. We can rewrite these terms in a more computationally efficient form by first writing the integral in the second term as a sum of integrals over unit cells and then using the periodicity of the denisty to find[13]

$$W_k = \int_V d\vec{r} \left[E_k[\rho_E(\vec{r})] - \sum_i \sum_{\vec{l}} E_k\left[\sum_{j=1}^{n_i} \rho_{ij}(\vec{r}-\vec{r}_{ijl})\right]\right] . \tag{5}$$

Each electron-gas interaction energy is calculated as a three-dimensional integration over a unit cell. Since the electronic densities fall off exponentially at long distance, the sums in ρ_E and in the second term of Eq. (7) converge rapidly.

2. Electrostatic energy

The total charge density can be expressed as

$$\rho_T(\vec{r}) = \sum_i \sum_{j=1}^{n_i} \sum_{\vec{l}} [Z_{ij}\delta(\vec{r}-\vec{r}_{ijl}) - \rho_{ij}(\vec{r}-\vec{r}_{ijl})] , \tag{6}$$

where Z_{ij} is the nuclear charge of the (ij)th center and $\delta(\vec{r})$ is the Dirac δ function. The total electrostatic potential

$$\Phi_T(\vec{r}) = \int d\vec{x}\, \rho_T(\vec{x})/|\vec{r}-\vec{x}|$$

can be written as

$$\Phi_T(\vec{r}) = \sum_i \sum_{j=1}^{n_i} \sum_{\vec{l}} \left[\frac{Z_{ij}}{|\vec{r}-\vec{r}_{ijl}|} - \Phi_{ij}(\vec{r}-\vec{r}_{ijl})\right] ,$$

where

$$\Phi_{ij}(\vec{r}) = \int d\vec{x}\, \rho_{ij}(\vec{x})/|\vec{r}-\vec{x}| .$$

The total electrostatic energy per unit cell can be written as[13]

$$W_T=\frac{1}{2}\sum_i\sum_{j=1}^{n_i}\int d\vec{r}\,[Z_{ij}\delta(\vec{r}-\vec{r}_{ij})-\rho_{ij}(\vec{r}-\vec{r}_{ij})]\Phi_T(\vec{r})\ . \tag{7}$$

It is convenient to introduce the terms Q_{ij}, the total number of electrons on each center, given by

$$Q_{ij}=\int d\vec{r}\,\rho_{ij}(\vec{r})\ , \tag{8}$$

and the total charge on each center N_{ij}, given by

$$N_{ij}=Z_{ij}-Q_{ij}\ . \tag{9}$$

The electrostatic interaction energy W_E is the total energy minus the molecular self-energy terms and can be written as

$$W_E=W_M+W_{\rm npc}\ ,$$

where, after integrating over the δ functions and rearranging we have

$$W_M=\frac{1}{2}\sum_i\sum_{j=1}^{n_i}\sum_m\sum_{p=1}^{n_m}{\sum_{\vec{l}}}'N_{ij}N_{mp}/|\vec{r}_{ij}-\vec{r}_{mpl}| \tag{10}$$

and

$$W_{\rm npc}=\frac{1}{2}\sum_i\sum_{j=1}^{n_i}\sum_m\sum_{p=1}^{n_m}{\sum_{\vec{l}}}'\left[N_{ij}G_{mp}(\vec{r}_{ij}-\vec{r}_{mpl})+N_{mp}G_{ij}(\vec{r}_{ij}-\vec{r}_{mpl})+\int d\vec{r}\,\rho_{ij}(\vec{r}-\vec{r}_{ij})[G_{mp}(\vec{r}_{ij}-\vec{r}_{mpl})-G_{mp}(\vec{r}-\vec{r}_{mpl})]\right]\ , \tag{11}$$

where

$$G_{ij}(r)=Q_{ij}/r-\Phi_{ij}(r)\ .$$

The prime on the sums over $\vec{l}$ indicates that the $i=m$ term is not included for $\vec{l}=0$. This restriction ensures that no interactions between centers on the same molecule will be included.

The term W_M is the form of the interaction energy of a lattice of point charges, the Madelung energy, appropriate for molecular crystals. We note that the evaluation of this term is an exact evaluation of the nonoverlap part of the electrostatic interaction in the molecular crystal, to any desired accuracy, for the given charge distribution. This term can be evaluated by a method based on the Ewald double-sum formula.[21] We have, following a derivation similar to that given by Muhlhausen and Gordon for monatomic crystals,[13]

$$\begin{aligned}W_M=&\frac{2\pi}{V}\sum_{\vec{k}}\left[\sum_i\sum_{j=1}^{n_i}N_{ij}e^{-i\vec{k}\cdot\vec{r}_{ij}}\right]\left[\sum_m\sum_{p=1}^{n_m}\frac{N_{mp}}{k^2}e^{i\vec{k}\cdot\vec{r}_{mp}}e^{-k^2/4\alpha_{mp}^2}\right]\\&+\frac{1}{2}\sum_i\sum_{j=1}^{n_i}\sum_m\sum_{p=1}^{n_m}{\sum_{\vec{l}}}'N_{ij}N_{mp}\,\mathrm{erfc}(\alpha_{mp}|\vec{r}_{ij}-\vec{r}_{mpl}|)/|\vec{r}_{ij}-\vec{r}_{mpl}|\\&-\frac{1}{2}\sum_i\sum_{j=1}^{n_i}\sum_{p=1}^{n_i}N_{ij}N_{ip}\,\mathrm{erf}(\alpha_{ip}|\vec{r}_{ij}-\vec{r}_{ip}|)/|\vec{r}_{ij}-\vec{r}_{ip}|\ ,\end{aligned} \tag{12}$$

where $\vec{k}$ is a reciprocal-lattice vector, V is the unit-cell volume, erf and erfc the error and complementary error functions, respectively, and α_{ij} a parameter chosen for quick convergence of the summations. The total electrostatic potential at a site is given by

$$\begin{aligned}\Phi_s(\vec{r}_{ij})=&\sum_m\sum_{p=1}^{n_m}{\sum_{\vec{l}}}'[G_{mp}(\vec{r}_{ij}-\vec{r}_{mpl})+N_{mp}\,\mathrm{erfc}(\alpha_{mp}|\vec{r}_{ij}-\vec{r}_{mpl}|)/|\vec{r}_{ij}-\vec{r}_{mpl}|]\\&+\frac{4\pi}{V}\sum_{\vec{k}}\frac{1}{k^2}\sum_m\sum_{p=1}^{n_m}(N_{mp}e^{i\vec{k}\cdot\vec{r}_{mp}}e^{-k^2/4\alpha_{mp}^2})e^{-i\vec{k}\cdot\vec{r}_{ij}}-\frac{\pi}{V}\sum_i\sum_{j=1}^{n_i}N_{ij}/\alpha_{ij}^2\ .\end{aligned}$$

The second term, W_{npc}, is the interaction energy due to the overlap of the charge distributions, the nonpoint Coulomb energy. This term can be evaluated in the method similar to that used by Muhlhausen and Gordon for atomic ionic crystals.[13] This method involves splitting the expression into a number of terms including summations in the direct and reciprocal lattices and an integration over the unit cell. Details of the formulation of this method for molecular crystals are given elsewhere.[22] We found that while this method worked well for crystals with small unit cells, there were convergence problems for large unit cells. For this reason, the nonpoint Coulomb energy was evaluated for crystals with four or more molecules per unit cell as a sum of pair interactions between the spherically symmetric functions representing the electron densities in separate molecules or ions [the term within the large parentheses in Eq. (11)]. The potentials between the different centers are calculated by a Gauss-Legendre quadrature at the beginning of the calculation and evaluated when needed by cubic-spline interpolation. Because the pair interaction terms go to zero exponentially, evaluation of this term by summing the pair interactions is about as time consuming as the more complicated method of Muhlhausen and Gordon.[13]

III. NUMERICAL INTEGRATION METHODS

The three-dimensional integrations over the unit cell can be performed with a number of techniques, such as by Gauss-Legendre quadratures. We have chosen, however, to take advantage of the periodicity of the integrand and use one of the "number-theoretic" methods which have been developed. In particular, we shall use a method taken from Conroy,[23] which is similar to methods proposed by Korobov[24] and Haselgrove.[25] In this method the integration is performed along vectors in the periodic space in directions which have been optimized by Conroy for given numbers of integration points. We find that we can get convergence of the integrations over the unit cell with either 1154 or 3722 total points, depending on the size of the unit cell and number of molecules in each unit cell.

The electron-gas terms in Eq. (5) involve an integration over the unit cell, and have integrands that are sharply peaked around the nuclei. In particular, the kinetic and exchange energy integrals have integrands that are generally quite small throughout the unit cell but that can increase by more than an order of magnitude near the nuclei. It is difficult to evaluate accurately the regions around the sharp peaks with numerical integration. In order to improve the accuracy of the numerical integration we replace the sharply peaked functions near the nuclei by a smoother function in a small sphere about the nuclei. A correction term is evaluated to account for the change of function. When this procedure is followed, the integration becomes numerically much more stable.[13]

The kinetic and exchange contributions to the interaction energy are of the form of Eq. (5),

$$I_n = C\int_V d\vec{r}\left[\sum_i\sum_{j=1}^{n_i}\sum_{\vec{l}}\rho_{ij}(\vec{r}-\vec{r}_{ijl})\right]^{n/3} - \sum_i\sum_{\vec{l}}\left[\sum_{j=1}^{n_i}\rho_{ij}(\vec{r}-\vec{r}_{ijl})\right]^{n/3} \equiv I_n[V,\rho]\ ,$$

where $n=5$ for the kinetic energy and 4 for the exchange.

We replace the highly peaked density ρ_{ij} by a smooth function f_{ij} in a small sphere V_{ij} of radius d_{ij} about each center in the unit cell and obtain the new density h_{ij},

$$h_{ij}(r)=\begin{cases}\rho_{ij}(r), & r\geq d_{ij}\\ f_{ij}(r), & r\leq d_{ij}\ .\end{cases}$$

The integral I_n becomes

$$I_n = I_n[V,h]+\sum_m\sum_{p=1}^{n_m}\left(-I_n[V_{mp},f]+I_n[V_{mp},\rho]\right)\ ,$$

where the latter terms correct for the replacement of the true integrand. The notation $[V,f]$ indicates to integrate over the volume V with the function f describing the density near the nuclei. Since it is assumed that the radius of the sphere around a center is small, the total density is expanded near a center about the density associated with that center.

We have found that when fitting a molecular density with spherical Slater functions, densities centered along the bond (between the nuclei) must be included to get good fits. However, the magnitude of the density near the origin of these bond charges is small and generally quite smooth. We can therefore expand the total density near the nuclei in a molecule in terms of small deviations

from the function centered on the nucleus. In general, no approximations to the integrand need be made for those centers not centered on the nuclei. Because of the spherical symmetry of the charge densities, the derivation of the correction terms is quite similar to that given previously for monatomic crystals.[13] We include the present derivation to show explicitly the assumptions made in the molecular case. We expand the total density near a center mp as

$$\rho_T(r)=\sum_i\sum_{j=1}^{n_i}\sum_{\vec{l}}\rho_{ij}(\vec{r}-\vec{r}_{ijl}+\vec{r}_{mp})$$
$$=\rho_{mp}(r)+\sum_i\sum_{j=1}^{n_i}\sum_{\vec{l}}{}''\rho_{ij}(\vec{r}-\vec{r}_{ijl}+\vec{r}_{mp}),$$

where the $''$ indicate only the $\vec{l}=0$, $i=m$, and $j=p$ term is omitted from the sum. By our earlier assumptions, we can take

$$b_{mp}=\sum_i\sum_{j=1}^{n_i}\sum_{\vec{l}}{}''\rho_{ij}(\vec{r}-\vec{r}_{ijl}+\vec{r}_{mp})/\rho_{mp}(r)$$

as small, and expand to find

$$\rho_T^{n/3}=\rho_{mp}^{n/3}(r)(1+b_{mp})^{n/3}$$
$$\approx\rho_{mp}^{n/3}(r)\left[1+\frac{n}{3}b_{mp}+\cdots\right].$$

We define

$$B=\sum_i\sum_{\vec{l}}\left[\sum_{j=1}^{n_i}\rho_{ij}(\vec{r}-\vec{r}_{ijl}+\vec{r}_{mp})\right]^{n/3}=\left[\sum_{j=1}^{n_m}\rho_{mj}(\vec{r}-\vec{r}_{mj}+\vec{r}_{mp})\right]^{n/3}+\sum_i\sum_{\vec{l}}{}'\left[\sum_{j=1}^{n_i}\rho_{ij}(\vec{r}-\vec{r}_{ijl}+\vec{r}_{mp})\right]^{n/3},$$

where the $'$ means no $i=m$ term for $\vec{l}=0$. Letting

$$g_{mp}=\sum_{j=1}^{n_m}{}''\rho_{mj}(\vec{r}-\vec{r}_{mj}+\vec{r}_{mp})/\rho_{mp}(r),$$

where the $''$ means no $j=p$ term and expanding the first term in B we find

$$I_n[V_{mp},\rho]\approx C\int_{V_{mp}}\frac{n}{3}\rho_{mp}^{n/3}(r)(b_{mp}-g_{mp})-\sum_i\sum_{\vec{l}}{}'\left[\sum_{j=1}^{n_i}\rho_{ij}(\vec{r}-\vec{r}_{ijl}+\vec{r}_{mp})\right]^{n/3}.$$

The last term is a sum over the densities due to other molecules evaluated near the mp center, which we assume are negligible with respect to ρ_{mp} and are dropped. We are left with

$$I_n[V_{mp},\rho]=\frac{nC}{3}\int d\vec{r}\,\rho_{mp}^{(n-3)/3}(r)\sum_i\sum_{j=1}^{n_i}\sum_{\vec{l}}{}'\rho_{ij}(\vec{r}-\vec{r}_{ijl}+\vec{r}_{mp}),$$

where the $'$ means no $i=m$ term for $\vec{l}=0$ in the summation. Since the summation contains terms that are centered on different molecules, we can write a Taylor-series expansion of these terms as

$$\rho_{ij}(\vec{r}-\vec{r}_{ijl}+\vec{r}_{mp})\approx\rho_{ij}(\vec{r}_{mp}-\vec{r}_{ijl})+\left.\frac{d\rho_{ij}}{dr}\right|_{r=|\vec{r}_{mp}-\vec{r}_{ijl}|}[\vec{r}\cdot(\vec{r}_{mp}-\vec{r}_{ijl})]/|\vec{r}_{mp}-\vec{r}_{ijl}|.$$

Since ρ_{mp} is spherically symmetric, an integration over the dot product is zero and we find

$$I_n[V_{mp},\rho]\approx\frac{nC}{3}\sum_i\sum_{j=1}^{n_i}\sum_{\vec{l}}{}'\rho_{ij}(\vec{r}_{mp}-\vec{r}_{ijl})\int_{V_{mp}}d\vec{r}\,\rho_{mp}^{(n-3)/3}(r).$$

Since the terms multiplying the integral are due to densities on other molecules, these correction terms are small. We have reduced the rather complicated correction integrals to sums of densities times integrals that have to be evaluated only once per center. The correction term $I_n[V_{mp},f]$ has the same form with f replacing ρ. We choose as the smoothing function

$$f_{ij}(r)=a_{ij}+b_{ij}r^2,\quad r\le d_{ij}$$

where the constants are chosen to fit the density and its first derivative at $r=d_{ij}$.

With this smoothing procedure and corresponding corrections the stability of the numerical integration over the unit cell is greatly improved. Muhlhausen and Gordon[13] provide a number of

numerical tests for atomic ionic crystals that show the improvement in the numerical integration found with this procedure. Details of the correction terms necessary for the numerical integration if the nonpoint Coulomb energy is not evaluated as a sum of pair integrations are available.[22]

IV. CRYSTAL CHARGE DENSITIES AND ENERGETICS

A. Charge densities

As outlined in Sec. II A, the electron-gas model takes as an approximation to the total electronic density of a system the sum of the densities of the component atoms and molecules, where for most systems the densities of the gas-phase molecules are used. One method to improve the model is to improve the description of the densities, keeping, if possible, the additive density approximation. The necessity of these improvements depends on how much the component densities differ from the densities of the gas-phase molecules.

For interacting neutral systems, the interactions between molecules are small unless the intermolecular distances are very small. For these systems, the deviation of the component densities from their gas-phase densities is small and a perturbative approach can be made. With this approach, very good results have been obtained with the electron-gas model for intermolecular potentials between neutral molecules.[10]

The component ions within ionic crystals, however, are subject to very strong electrostatic potentials and potential gradients. These potentials can cause relatively large distortions in the electronic distributions of the ions. In monatomic ions, the usual approach to treating these distortions has been to consider two effects, an isotropic compression or expansion of the ions and an asymmetric distortion due to field gradients. For monatomic ionic crystals with high symmetry, the compression of the negative ions seems to be the dominant effect. Muhlhausen and Gordon,[13] following the work of Watson[16] and Pachalis and Weiss,[17] approximated this compression by adding a term to the atomic Hamiltonian corresponding to the potential due to an external shell of charge. The charge density of this system is found with the Hartree-Fock SCF method. In the Muhlhausen-Gordon model, the charge on the external shell was taken to be the opposite of the charge on the ion it surrounds (for system neutrality). The radius of the shell was chosen to match the potential due to the shell at the ion's nucleus with the potential at that nucleus due to all charges in the crystal other than the ion itself (site potential). With the use of these stabilized densities, significant improvements in the agreement between the calculated and experimental crystal properties were obtained.

In molecular ionic crystals, there is no simple analog to the atomic case, since there cannot be a simple isotropic change in the density. We can, however, approximate the effects of the crystal environment by adding to the molecular Hamiltonian terms corresponding to the interaction with a set of external point charges, chosen in such a way as to match the site potential in the crystal. In particular, we match the site potential found at each center along the bond in the molecular ion with a set of six external charges, chosen to keep the axial symmetry of the molecules. For molecules oriented along the z axis, the six charges would be located at $(0,0,z_1)$, $(0,0,-z_2)$, $(\pm a,0,b)$, and $(0,\pm a,b)$ with charges q_1, q_2, and q_a, respectively. The sum of the external charges $(q_1+q_2+4q_a)$ is chosen to be opposite the charge on the molecule or ion. The parameters z_1, z_2, a, b, q_1, and q_2 were found by a nonlinear least-squares fit to the crystal site potential. For example, for LiOH discussed below, the crystal site potentials were found to be 0.474, 0.462, 0.449, and 0.322, while the potentials due to the set of external charges were 0.458, 0.463, 0.461, and 0.319 at the positions along the bond [−0.2, 0.0 (O atom), 0.2, 1.8557 (H atom)]. The parameters were −4.545, 4.785, 1.302, 0.12, 0.440, and 0.112, respectively. The electronic densities were found by use of the Hartree-Fock SCF method on the molecular ion plus the external charges.

The calculations on the molecular ions were performed using the POLCAL program of Stevens.[26] Since the external charges have no electrons or orbitals associated with them, inclusion of these charges has little effect on the running time of the SCF calculations. To preserve cylindrical symmetry, only s and p functions are used.

The energy of the stabilized ion (E_s) can be found by subtracting from the total SCF energy of the system (molecular ion plus external charges) the interaction between the external charges and the electrons and nuclei of the molecule, as well as the interactions between the external charges. The difference between the SCF energy of the gas-phase ion (E_g) and the stabilized ion is the stabilization energy ΔE_s:

$$\Delta E_s = E_s - E_g \ . \tag{13}$$

B. Crystal energies

The total crystal binding energy per formula unit W_B is given in Eqs. (1), (5), (11), and (12). This energy can be minimized with respect to the lattice parameters of the unit cell and the positions and orientations of the molecule in the unit cell. We find the optimal stabilization by an iterative process. First the lattice energy is minimized using an electronic density for the gas-phase molecular ion. The site potentials along the molecular bond found in this calculation are matched by the potentials due to a set of external point charges. An SCF calculation is then performed on the combined system. The resultant wave function is used to find the molecular density which is then fit to a sum of spherical Slater functions as described in Sec. II B and another minimization of the crystal binding energy is performed. The site potentials found at this minimum are compared with those due to the external charges that stabilized the ion. If the deviation between the two sets of potentials is less than a few percent, we stop the process. If not, the new site potentials are matched by external charges and the steps are repeated until there is agreement between site potentials in successive calculations. In practice, self-consistency is obtained with no more than one or two iterations. The binding energy of the self-consistent calculation is E_B.

The dissociation energy of the crystal is defined as the process of going from ions in the crystal to free ions in the gas phase. Since the binding energy we calculate is the energy of the ions in the crystal going to stabilized ions, the dissociated energy is given by

$$D_e = -E_B - m\Delta E_s \ ,$$

where m is the number of formula units of the stabilized ion in the ionic molecule. The iterative scheme is a minimization of this dissociation energy. As the molecules are stabilized, their size shrinks. The molecules in the crystal can then get closer together and the binding energy increases in magnitude. The stabilization energy also increases in size as the molecules are further stabilized. As the signs of the two energies are opposite, there is a minimum in the dissociation energy curve. Because the dissociation energy curve is flat near the minimum, and there are inaccuracies in the energy, it is not possible to find the best wave function for the crystal of interest. The point of self-consistency is used as a good approximation to the true minimum.[13]

V. ALKALI AND ALKALINE-EARTH HYDROXIDES

A crucial test for any theory of molecular crystals is that it be able to account not only for general structural features such as lattice size, but also the relative positions and orientations of the atoms and molecules in the crystals. These orientations depend not only on the long-range interactions but the short-range interactions as well. Theoretical predictions of hydrogen positions have been made for a number of hydroxide crystals,[27,28] but they have neglected completely the effects of the short-range forces. Here we apply the theory to a series of crystals involving hydroxide ions, the alkali and alkaline-earth hydroxides. In particular, we shall examine the success of the model in predicting structures and energies, as well as the relative importance of the dipolar versus repulsive forces in determining the hydroxide orientations. The partitioning of the energy into long- and short-range contributions will be discussed in detail for $Mg(OH)_2$ crystals.

The model used has been outlined in Secs. II–IV. The correction factors for the MEG theory (Sec. II A) were taken as appropriate for the nearest-neighbor pair. For example, for NaOH the correction factors for 20 electrons (16 valence) were used and for KOH those for 28 electrons (16 valence) were used. In the case for NaOH, the correction factors are appropriate for all pairs in the crystal, while for KOH the correction factors used are intermediate between those appropriate for the K-K and OH-OH interactions. As noted by Muhlhausen and Gordon,[13] the results are not very dependent on the choice of correction factors.

The electronic density of the gas-phase OH^- ion used in the first step of the iteration cycle was calculated from the wave function of Cade, which was better than a double-ζ wave function with added p- and f-polarization functions.[29] This wave function gives energies close to the Hartree-Fock limit. Some molecules properties calculated with this wave function are given in Table I.

The wave function used to calculate the stabilized molecular densities had the same basis as the gas-phase wave function of Cade but without the added d and f functions. These functions were dropped to preserve cylindrical symmetry in the Hartree-Fock SCF calculations which included the external charges. As a check of the basis set, partial optimization of exponents were carried out in a calculation of the gas-phase ion. The SCF energy and dipole and quadrupole moments are given for

TABLE I. Comparison of OH^- properties. All quantities are in atomic units. The OH bond length is R_{OH} and the SCF energy (after subtracting the interactions with any external charges) is E_{SCF}. The electrostatic moments μ (dipole) and ϑ (quadrupole) refer to the oxygen atom with a molecular orientation O-H.

Wave function	R_{OH}	μ	ϑ	E_{SCF}
SCF[a]	1.781	0.4289	1.9321	−75.417 54
OH^- (1)[b]	1.8557	0.5067	1.9526	−75.407 62
OH^- (2)	1.8557	0.6597	1.7574	−75.379 08
OH^- (3)	1.8557	0.6336	1.8101	−75.394 96
OH^- (4)	1.8557	0.6521	1.6743	−75.377 36
OH^- (5)	1.8557	0.6124	1.8063	−75.399 19
OH^- (6)	1.8557	0.7099	1.8751	−75.386 97

[a]Reference 29.

[b]The wave function OH^- (1) is the present free-molecule wave function. The others are the wave functions used to calculate the electronic density for the calculations on: (2) LiOH, (3) NaOH, and $Sr(OH)_2$; (4) $Mg(OH)_2$, (5) KOH, and RbOH; and (6) $Ca(OH)_2$.

comparison with the result of Cade in Table I. The bond length used in the present calculation was from crystal x-ray diffraction data. The stabilized wave functions were generated as described in Sec. IV. The exponents were optimized for one stabilization and used in all subsequent calculations. Selected molecular properties as calculated from these wave functions are given in Table I. Molecular electronic densities were fit to four spherical functions centered along the bond with relative standard deviations in the fits of about 3%. Four centers were the minimum number found to give a reasonable representation of the molecular densities. Convergence of the interaction cycle is shown in detail for the case of NaOH. All charge densities for the positive ions were calculated from available wave functions.[30,31]

1. LiOH

The structure of LiOH has been determined by neutron diffraction to be tetragonal with two molecules per unit cell (space group of $P4/nmm$).[32] The experimental parameters are given in Table II, where the lithium atoms are in positions $\pm(\frac{1}{4},\frac{1}{4},0)$, the O and H atoms in $\pm(\frac{1}{4},\frac{3}{4},z)$, and the structure shown in Fig. 1.

The lattice energy was minimized with respect to the parameters a, c, and z_0, with the lithium ions and hydroxide orientations fixed. As a check of the structure, the orientations of the hydroxide ions were varied, with the most favored structure being that shown in Fig. 1. The calculated properties are given in Table II and compared with the experimental results. The calculated dissociation energy is within the experimental error and the lattice parameters within 2% of those determined at 298 K.

In Table I are listed the molecular properties of the wave function used for the converged result for LiOH. The dominant change of the crystalline hydroxide ion relative to the free molecule is an increase in the dipole moment relative to the oxygen atom, indicating a shift in electronic density towards the oxygen atom.

2. NaOH

Three modifcations for NaOH are known; the low-temperature ($T < 573$ K) orthorhombic phase, the α phase, and higher-temperature monoclinic and cubic phases.[33] The structure of the α phase has been determined by neutron diffraction[33] to have four molecules per unit cell with space-group $Bmmb$ and special positions

$$\pm(\tfrac{1}{4},\tfrac{1}{4},z);(\tfrac{3}{4},\tfrac{3}{4},\tfrac{1}{2}+z)\,.$$

The structure is shown in Fig. 2 and the experimentally determined lattice parameters and energy in Table II.

In Table II are listed the results of calculations with the gas-phase wave function of Cade[31] and two stabilized wave functions, where the lattice parameters a and c and the positional parameters

TABLE II. Results for LiOH, NaOH, $Mg(OH)_2$, and $Ca(OH)_2$. All quantities are in atomic units. The lattice parameters are a and c, the positional parameters of the metal and oxygen atoms are denoted by z_m and z_O, respectively, the crystal electrostatic site potentials at the O and H atoms are Φ_O and Φ_H, respectively, the energy to separate the crystal to stabilized atoms and molecules is $-E_b$, and the crystal dissociation energy is D_e. The wave functions used here are denoted by OH^- (2), etc., and properties of these functions are given in Table I.

	a	c	z_m	z_O	Φ_O	Φ_H	$-E_b$	D_e
LiOH:								
free ion	7.356	7.754		0.162	0.433	0.327	0.3728	0.3728
OH^- (2)	6.716	8.645		0.166	0.464	0.333	0.4187	0.3903
experiment[a]	6.709	8.183		0.194				0.3888[b]
NaOH:								
free ion	6.879	22.442	−0.086	0.116	0.364	0.315	0.3182	0.3182
stabilized OH^-	6.672	22.442	−0.089	0.114	0.376	0.311	0.3307	0.3248
OH^- (3)	6.502	22.221	−0.090	0.114	0.383	0.318	0.3460	0.3334
experiment[c]	6.424	21.499	−0.086	0.116				0.3382[d]
$Mg(OH)_2$:								
free ion	6.521	8.874		0.222	0.445	0.292	1.0267	1.0267
OH^- (4)	6.088	9.549		0.192	0.469	0.313	1.1544	1.0939
experiment[e]	5.938	9.006		0.222				1.1333[f]
$Ca(OH)_2$:								
free ion	7.142	9.673		0.189	0.395	0.262	0.9722	0.9722
OH^- (6)	6.946	9.144		0.218	0.414	0.283	1.0391	0.9978
experiment[g]	6.777	9.221		0.235				0.9961[h]

[a]Reference 32 at 298 K.
[b]Reference 42 at 0 K. The uncertainty is about ±0.0016.
[c]Reference 33 at 298 K.
[d]Reference 42 at 0 K. The uncertainty is about ±0.0016.
[e]Reference 34 at 298 K.
[f]References 43 and 42 at 0 K. The uncertainty is about ±0.0037.
[g]Reference 39 at 298 K.
[h]References 43 and 42 at 0 K. The uncertainty is about ±0.0033.

z_{Na} and z_O were varied. The orientations of the hydroxides were checked and found to favor the orientations shown in Fig. 2. Also given in Table II are the calculated crystal site potentials and the potentials from the external charges in the stabilization calculation. Examination of the dipole moment given in Table I shows that there is a shifting of the electronic density towards the oxygen atom as the molecules are stabilized. As the wave function is stabilized by larger potentials from external charges, the spatial extent of the wave function decreases and the crystal can pack more tightly. The increased binding energy from this more tightly packed crystal is offset by the energy necessary to stabilize the OH^- molecule and cause a shift in the electronic density.

3. $Mg(OH)_2$

The crystal structure of $Mg(OH)_2$ (Brucite) has been determined by neutron diffraction as hexagonal with one molecule per unit cell and space group $P\bar{3}m\,1$.[34] The crystal structure is shown in Fig. 3 and corresponds to having atoms in the special positions

$$Mg^{2+}:\ (0,0,0)\,,$$

$$O(H):\ \pm\left(\tfrac{1}{3},\tfrac{2}{3},z\right)\,,$$

with the orientations of the hydroxides as shown in Fig. 3 and the oxygen positions as listed in Table II.

The results from calculations on the $Mg(OH)_2$

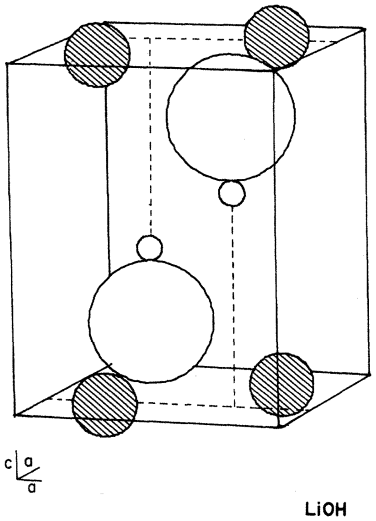

FIG. 1. Crystal structure (Ref. 32) of LiOH. The shaded spheres are the Li atoms, the large open spheres are O atoms, and the small open spheres are the H atoms.

crystal are given in Table II. The agreement with experiment is reasonable (within about 3.3% in lattice parameters and 3.5% in dissociation energy) though the error is somewhat larger than for some

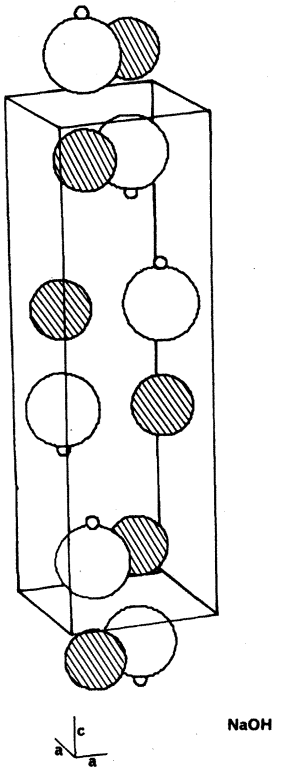

FIG. 2. Crystal structure (Ref. 33) of NaOH. The shaded spheres are the Na atoms, the large open spheres are O atoms, and the small open spheres are the H atoms.

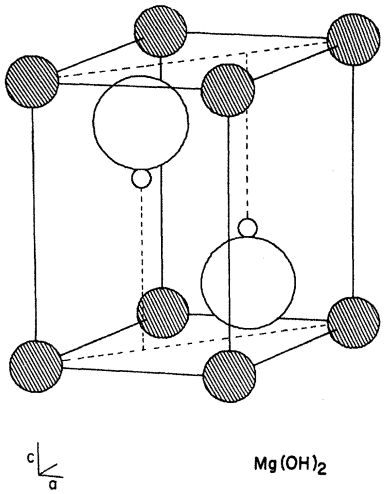

FIG. 3. Crystal structure (Ref. 34) of $Mg(OH)_2$ and (Ref. 39) of $Ca(OH)_2$. The shaded spheres are the Mg(Ca) atoms, the large open spheres are O atoms, and the small open spheres are the H atoms.

of the other hydroxide systems studied.

To examine the relative importance of the electrostatic and repulsive forces in determining the orientations of the hydroxide molecules, a calculation was performed in which all molecules and atoms but one were fixed in the theoretical minimum position and one molecule rotated about the O atom in the xz plane. The energy curves from this calculation are shown in Fig. 4, where

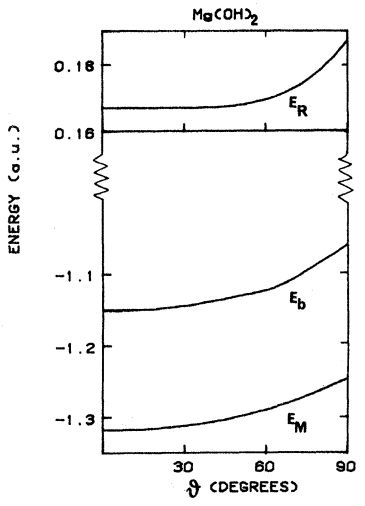

FIG. 4. Variation of energy of $Mg(OH)_2$ as a function of rotation of the hydroxide ion (with $z_0=0.222$) in the ac plane. ϑ is the angle between the orientation vector of the hydroxide ion and the c axis. E_M is the Madelung energy, E_b the binding energy, and E_R the total short-range repulsive energy.

the electrostatic, repulsive, and total energies are shown as a function of angle of hydroxide orientation relative to the z axis, ϑ. While the electrostatic forces dominate in determining the preferred orientation, the short-range forces have a decided influence on the shape of the energy surface, especially at large ϑ.

Since we find reasonably good agreement with the experimental results using a completely ionic model, this suggests that the covalent nature of the bonds is small. This view is supported by recent work by Haycock *et al.*,[35] who studied $Mg(OH)_2$ with x-ray emission, x-ray photoelectron, and Auger spectroscopy and report that the spectra indicate the strongest interaction is between the O and H atoms of the hydroxyl group. They do suggest, however, that there is some covalent character to the Mg^{2+}-O atom interactions and some hydrogen bonding between layers of the brucite structure. From our reasonably close agreement with experiment, these covalent effects seem to be much less important than the ionic forces and the shifting in electronic density due to the strong electrostatic potentials, though they could account for the somewhat larger errors in our $Mg(OH)_2$ calculations.

4. KOH

The two known phases of solid KOH are the monoclinic α phase and the higher-temperature ($T > 517$ K) cubic β phase.[36,37] The α phase has been studied at room temperature by x-ray diffraction[37] and at 93 K by infrared spectroscopy[38] by Ibers *et al.*, with the experimental parameters given in Table III. X-ray powder patterns at 140 K indicated that the room-temperature structure remained at the lower temperature. While they could not positively assign the hydrogen positions

TABLE III. Results for KOH, RbOH, and $Sr(OH)_2$. All quantities are in atomic units. Notation is as in Table II.

	a	b	c	β	Φ_O	Φ_H	$-E_b$	D_e
KOH:								
OH^- (5)[a]	7.185	7.276	12.290	106.7	0.347	0.301	0.3109	0.3025
experiment[b]	7.483	7.446	10.715	105.9				0.3020[c]
RbOH:								
OH^- (5)[d]	7.606	7.500	12.521	107.3	0.327	0.282	0.3007	0.2923
experiment[b]								0.2944[e]
$Sr(OH)_2$:								
OH^- (7)[f]	17.823	11.605	7.420		0.389	0.278	0.9823	0.9570
experiment[g]	18.688	11.567	7.405					0.9416[c]

[a]The positional parameters found here are: K^+: (0.144,$\frac{1}{4}$,0.290), O: (0.374,$\frac{1}{4}$,0.750), H: (0.456,0.25,0.907).

[b]Reference 37 at 298 K. The heavy-atom positions are reported as K^+: (0.175,$\frac{1}{4}$,0.288) and O: (0.318,0.25,0.770).

[c]Reference 42 at 0 K. The uncertainty is about ± 0.0016.

[d]The positional parameters found here are Rb^+: (0.143,$\frac{1}{4}$,0.293), O: (0.377,$\frac{1}{4}$,0.751), and H: (0.523,0.25,1.044).

[e]Reference 44 at 298 K. The uncertainty is about ± 0.0033.

[f]The Sr^{2+} positions were kept at the experimental values. The hydrogen atom positions were found to be: H (1): (0.422,0.198,$\frac{1}{4}$) and H (2): (0.473,0.859,$\frac{1}{4}$). The oxygen positions were found as O (1): (0.400,0.354,$\frac{1}{4}$) and O (2): (0.369,0.859,$\frac{1}{4}$). The site potentials given here are the average of the values for molecule types 1 and 2.

[g]Reference 40 at 298 K. The heavy-atom positions are reported as Sr^{2+}: (0.161,0.096,$\frac{1}{4}$), O (1): (0.395,0.344,$\frac{1}{4}$), and O (2): (0.369,0.865,$\frac{1}{4}$). The hydrogen-atom positions suggested in Ref. 27 are: H (1): (0.396,0.186,$\frac{1}{4}$), H (2): (0.462,0.815,$\frac{1}{4}$).

from the single-crystal x-ray data, packing arguments and analysis of the infrared spectra could be used to infer likely positions.

The structure of the KOH crystal, giving the positions of the potassium and oxygen atoms, is shown schematically in Fig. 5(a). The heavy atoms are in special positions

$$(x,y,z);(\bar{x},\tfrac{1}{2}+y,\bar{z})$$

with the oxygen atoms aligned in the zig-zag chain shown in Fig. 5(b). From structural analysis, Ibers *et al.* suggest that the hydrogen atoms are in one of the structures shown in Fig. 5(c), with structure 2 most consistent with the vibrational spectra. From analysis of the spectra, an O-H—O-O angle of $4°\pm2°$ is suggested. This structure, where the O-H—O-O angle is set to 0°, is shown in Fig. 6(a).

We determined the crystal structure by minimizing the binding energy with respect to the lattice parameters (a,b,c,β), the positional parameters for K^+ and OH^-, and the orientation of the hydroxide ions. The structure found with this minimization is shown in Fig. 6(b) and the parameters given in Table III. Comparison of the experimental structure with the calculated structure shows rather large differences. While the calculated dissociation energy is in good agreement with experiment, the angle between the a and c axes is somewhat too large in the present calculation as is the c axis. The volume of the calculated phase is, however, in better agreement with an error of about 2.6% (0.7 cm^3/mole). The real nature of the discrepancy is shown in comparison of the structures in Fig. 6. The orientations of the hydroxide ions found here (perpendicular to the O-O zigzag chain) is quite different from that suggested by the experimental study. As a test of this large difference, a calculation was performed where the energy was minimized with all the heavy-atom positions and lattice parameters held constant and just the orientations of the OH^- ions varied. The energy minimum was found with the hydroxides at an intermediate orientation between that suggested by the experimental study and the theoretical minimum found here, with an O-H—O-O angle of about 23° (as opposed to the 4° that Ibers *et al.* suggest[37,38]). The difference in energy between the theoretical minimum [Fig. 7(b)] and the calculation where only the orientations were varied is about 0.3 kcal/mole and that between the theoretical minimum and the experimental structure about 0.6 kcal/mole, indicating that the energy surface of this crystal is very flat.

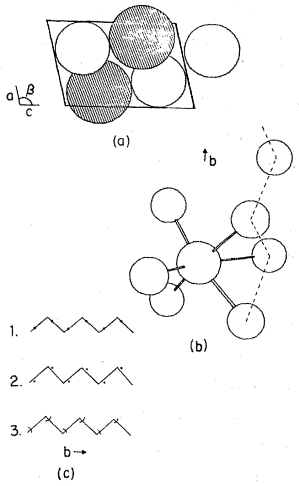

FIG. 5. From Ref. 37. (a) Projection of the KOH structure on the *ac* plane. The shaded spheres are the K atoms and the open spheres the O atoms. (b) View of the oxygen octahedron surrounding the K atoms showing the O-O zigzag chain. (c) Sketch of possible H atom positions along the chain of O atoms.

Because of the differences between experiment and theory in the case of KOH, the structure was calculated with two representations of the stabilized electronic density of the OH^- ion. The preliminary calculations were performed with an electronic density of OH^- calculated from a 3.7% fit of the stabilized wave function. The results were checked at the theoretical minimum by a calcula-

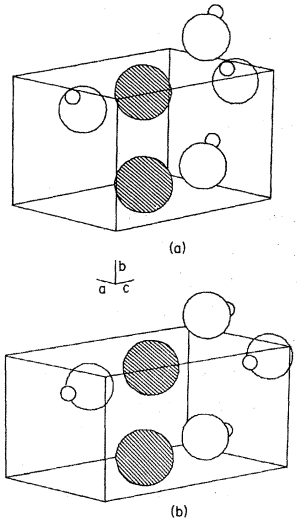

FIG. 6. Structure of KOH. The shaded spheres are the K atoms, the large open spheres are O atoms, and the small open spheres are the H atoms. (a) From Ref. 37. The hydrogen atom positions are placed along the O-O zigzag chain. (b) Present results.

tion using a more accurate representation of the hydroxide density with a relative standard deviation of about 0.3%. The difference in dissociation energy as calculated with the two representations is about 0.0028 a.u. (0.9%). The dissociation energy in Table III was found with the more accurate representation of the density at the positions found with the 3.7% fit.

The structure proposed in the experimental study is surprising in that a ferroelectric ordering of the hydroxide ions [Fig. 6(a)] is predicted. Our results [Fig. 6(b)] predict a structure in which the hydroxides have antiferroelectric (dipolar) ordering. The energy of these two structures is quite similar; however, at low temperature the present structure should be favored. This structure could be checked by infrared polarization studies on single crystal, which should show no hydroxide absorption along the crystal axis parallel to the hydroxide-ion orientations.

5. $Ca(OH)_2$

The crystal structure of $Ca(OH)_2$ (portlandite) is the same as that for $Mg(OH)_2$ discussed above.[39] The structure is shown in Fig. 3 and the results for $Ca(OH)_2$ are given in Table II. The present results are quite good with a relative standard error of about 1.32% in lattice constants and 1.5% in dissociation energy.

6. *RbOH*

Ibers *et al.* report that on the basis of an x-ray powder pattern RbOH is isostructural with KOH,[37] though no other information on values of the lattice constants is available. Calculations were performed on RbOH in the structure found above for KOH and a minimum was found with the structure as given in Fig. 6(b) with parameters as in Table III. We note that the same orientations were found for the OH^- ions as in the KOH crystals. The agreement with the experimental dissociation energy is good (0.7%).

7. $Sr(OH)_2$

The room temperature of $Sr(OH)_2$ has been studied with x-ray diffraction.[40] Because of the low scattering of the hydrogen atoms, their positions were estimated by packing arguments. In an infrared study of $Sr(OH)_2$ and $Ba(OH)_2$, further information about the hydrogen positions was obtained.[41] Perhaps the best indication of the hydroxyl orientations comes from a theoretical study by Giese,[27] who used an electrostatic model to examine a series of orientations. The experimental structure was determined to be orthorhombic with a space group of *Pnam* and four molecules per unit cell. The heavy atoms are in the special positions (x,y,z); $(\frac{1}{2}+x,\frac{1}{2}-y,z)$; $(\bar{x},\bar{y},\bar{z})$; $(\frac{1}{2}-x,\frac{1}{2}+y,\bar{z})$. The experimental parameters and the orientations predicted by Giese are given in Table III.

The results of our calculations are given in Table III and the structure in Fig. 7. Comparison with the experimental lattice parameters and energy show a reasonable agreement with an average error in lattice parameter of about 1.7% and dissociation energy of about 1.6%. The orientations found here are quite similar to those found in the study of Giese using an electrostatic model. These calculations were performed with a fit of the electronic density with a relative standard deviation of about 0.4%.

8. *Discussion*

A summary of the results of the calculations on the alkali and alkaline-earth hydroxide crystals is given in Table IV. Listed in this table are the percent errors with respect to the experimental results for the zero-pressure molar volumes, lattice parameters (averaged for each compound), and the dissociation energy. Most of the molar volumes determined here are larger than the experimental volumes, while the errors in dissociation energies are somewhat random. For all cases in which there is a significant ($>1\%$) error in the dissocia-

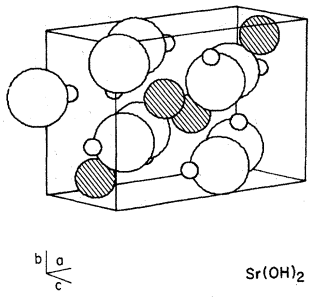

FIG. 7. Structure of $Sr(OH)_2$ with heavy-atom positions from Ref. 40 and hydrogen-atom positions from the present results. The shaded spheres are the Sr atoms, the large open spheres are O atoms, and the small open spheres are the H atoms.

TABLE IV. Summary of OH^- results. The errors given are percent deviations from the experimental values reported in the text. The average of the errors in the unit-cell parameters is $\Delta\%\langle|l|\rangle$, that of the molar volume is $\Delta\%V$, and that of the dissociation energy is $\Delta\%D_e$.

Crystal	$\Delta\%\langle\|l\|\rangle$	$\Delta\%V$	$\Delta\%D_e$
LiOH	2.0	5.9	0.4
NaoH	1.9	5.9	−1.4
$Mg(OH)_2$	3.7	11.5	−3.6
KOH	4.1	3.6	0.2
$Ca(OH)_2$	1.3	2.3	0.2
RbOH			−0.7
$Sr(OH)_2$	1.7	−4.1	1.6
Absolute error	2.5	5.6	1.1

tion energy, the errors in energy and volume have the opposite sign. This anticorrelation is expected, since if, for example, the short-range forces are overestimated, the lattice expands ($\Delta V > 0$) and the electrostatic binding energy decreases in size ($\Delta D_e < 0$). Overall, there is an average error of 5.6% in molar volume, 2.5% in lattice parameters, and 1.1% in dissociation energy.

There are a number of effects that contribute to error in the theory. For one thing, dispersion energies are only partially accounted for by inclusion of the correlation energy in the GK functional (Sec. II A). The correlation functional gives incorrect long-range behavior (exponential instead of $1/R^6$) and therefore underestimates the attractive forces. The neglect of these forces is partially canceled by a neglect of the vibrational zero-point energy. Muhlhausen and Gordon[13] found for cubic crystals that the neglect of the dispersion energy gave an error of less than 10 kcal/mole, which was mostly canceled by the zero-point energy, except for heavier systems (e.g., MgO and CaO). Other error comes from the error in the representation in the electronic density in the calculations. There are two parts to this error. First, the system of six external charges in the Hartree-Fock calculation only partially accounts for the true crystal environment. Inclusion of repulsive forces and a better description of the crystal site potential may change the electronic densities somewhat. Also, for most of the calculations on the hydroxide crystals, fits of the stabilized wave functions to about 3−4% were used. The results for the KOH crystal suggest that use of a better fit would change the calculated results by about 1%.

For all crystal systems studied, a change in the dipole moment of the hydroxide ion consistent with a shift in the electronic density towards the oxygen atom was observed. These changes in dipole moment ranged from about 20 to 40% of the free-molecule value. Anderson and Santry found similar changes (about 20%) in the molecular dipole moments in solid HF and HCL using an SCF perturbative approach.[15(b)] These changes in molecular properties due to the crystal environment suggest that theories of molecular solids that depend on gas-phase densities may be significantly in error.

VI. SUMMARY AND CONCLUSIONS

The electron-gas theory for molecular crystals presented here has been shown to give good agreement with the lattice geometries, hydroxyl orientations, and dissociation energies of the alkali and alkaline-earth hydroxides. Partial inclusion of the effects of the crystalline environment on the electronic distributions, through a simple electrostatic model, gives great improvement over calculations with gas-phase free-ion distributions and provides a way to study the effects of the crystalline environment on molecular properties. In particular, the electrostatically induced contraction of the negative (hydroxide) ionic densities results in contraction of the theoretical lattice size and an increase in binding energy, relative to the use of a free-ion wave function. Additional contraction effects on the electronic distributions due to Pauli repulsion from neighboring ions were not considered. Thus, the model still tends to give unit cells that are slightly too large. Inclusion of dispersion energies and the vibrational zero-point motion is expected to improve the results.

The orientations of the hydroxyl molecules in the alkali and alkaline-earth hydroxides have been found to be determined mainly by the dipolar electrostatic forces. The site potential due to the other atoms and molecules tends to increase the dipole moment of the OH^- ion relative to the O atom, indicating a shift in electronic density towards the oxygen atom. This increase in dipole causes increased stabilization of the crystal due to larger electrostatic forces.

ACKNOWLEDGMENTS

One of us (R.L.) would like to thank Dr. Carl Muhlhausen for many hours of discussion about the intricacies of the electron-gas model. We are grateful to Dr. Richard M. Stevens for the use of his molecular SCF program and the help he gave in its use. This work was supported by the National Science Foundation, Grants Nos. CHE80-15804 and EAR80-06535.

*Present address: Los Alamos National Laboratory, P. O. Box 1663, Los Alamos, NM 87545.

[1]A. I. Kitaigorodsky, *Molecular Crystals and Molecules* (Academic, New York, 1973); M. Born and K. Huang, *Dynamic Theory of Crystal Lattices* (Oxford University Press, London, 1954); M. P. Tosi, in *Solid State Physics,* edited by F. Seitz and D. Turnbull (Academic, New York, 1964), Vol. 16, p. 1.

[2]For example, M. Ross, J. Chem. Phys. 60, 3634 (1974).

[3]J. C. Raich and N. S. Gillis, J. Chem. Phys. 66, 846 (1977).

[4]R. B. Gerber, V. Buch, U. Buck, G. Maneke, and J. Schleusner, Phys. Rev. Lett. 44, 1397 (1980); R. B. Gerber, V. Buch, and U. Buck, J. Chem. Phys. 72, 3596 (1980).

[5]For example, T. Kihara, Rev. Mod. Phys. 25, 831 (1953); 27, 412 (1955).

[6]F. Muldar, G. van Dijk, and A. van der Avoird, Mol. Phys. 39, 407 (1980).

[7]For example, T. Luty, A. van der Avoird, and R. M. Berns, J. Chem. Phys. 73, 5305 (1980); R. D. Etters, R. Danilowicz, and W. England, Phys. Rev. A 12, 2199 (1975).

[8]R. G. Gordon and Y. S. Kim, J. Chem. Phys. 56, 3122 (1972).

[9]Y. S. Kim and R. G. Gordon, J. Chem. Phys. 60, 1842 (1974).

[10]M. Waldman and R. G. Gordon, J. Chem. Phys. 71, 1325 (1979).

[11]Y. S. Kim and R. G. Gordon, Phys. Rev. B 9, 3548 (1974).

[12]A. J. Cohen and R. G. Gordon, Phys. Rev. B 12, 3228 (1975); 14, 4593 (1976).

[13]C. Muhlhausen and R. G. Gordon, Phys. Rev. B 23, 900 (1981).

[14]L. L. Boyer, Phys. Rev. Lett. 42, 584 (1979); 45, 1858 (1980).

[15](a) J. L. Calais, Int. J. Quant. Chem. Symp. 9, 497 (1975); (b) S. G. Anderson and D. P. Santry, J. Chem. Phys. 74, 5780 (1981).

[16]R. E. Watson, Phys. Rev. 111, 1108 (1958).

[17]E. Pachalis and A. Weiss, Theor. Chim. Acta 13, 381 (1969).

[18]S. Green and R. G. Gordon, Program No. 251 (1974), Quantum Chemistry Program Exchange, University of Indiana, Bloomington, IN 47401.

[19]G. A. Parker, R. L. Snow, and R. T. Pack, Program No. 305 (1976), Quantum Chemistry Program Exchange, University of Indiana, Bloomington, IN 47401.

[20]G. A. Parker, R. L. Snow, and R. T. Pack, Chem. Phys. Lett. 33, 399 (1975).

[21]P. P. Ewald, Ann. Phys. (Leipzig) 64, 253 (1921); J. C. Slater, *Quantum Theory of Molecules and Solids* (McGraw-Hill, New York, 1967), Vol. 3, pp. 215–9.

[22]R. LeSar, Thesis (Harvard University, Cambridge, 1981) (unpublished).

[23]H. Conroy, J. Chem. Phys. 47, 5307 (1967).

[24]See A. H. Stroud, *Approximate Calculations of Multiple Integrals* (Prentice-Hall, Englewood Cliffs, New Jersey, 1971), Chap. 6 and references therein.

[25]C. B. Haselgrove, Math. Computation 15, 323 (1961).

[26]R. M. Stevens, J. Chem. Phys. 61, 2086 (1974).

[27]R. F. Giese, Z. Kristallogr. 146, 205 (1977).

[28]W. H. Bauer, Acta. Crystallogr. Sect. B 28, 1456 (1972).

[29]P. E. Cade, J. Chem. Phys. 47, 2390 (1967).

[30]E. Clementi and C. Roetti, At. Data Nucl. Data Tables 14, 177 (1974).

[31]C. Muhlhausen and R. G. Gordon, Phys. Rev. B 24, 2147 (1981); Ref. 12.

[32]H. Dachs, Z. Kristallogr. 112, 60 (1959).

[33]H. Stehr, Z. Kristallogr. 125, 332 (1967).

[34]F. Zigan and R. Rothbauer, Neus. Jahr. Mineralg. Monatschefte 4-5, 137 (1967).

[35]D. Haycock, M. Kasrai, C. J. Nicholls, and P. Urah, J. Chem. Soc. Dalton Trans. 12, 1791 (1978).

[36]C. Bec, J.-J. Counioux, G. Papin, and A. Scbaoun, C. R. Acad. Sci. Ser. C 278, 1193 (1974).

[37]J. A. Ibers, J. Kumamoto, and R. G. Snyder, J. Chem. Phys. 33, 1164 (1969).

[38]R. G. Snyder, J. Kumamoto, and J. A. Ibers, J. Chem. Phys. 33, 1171 (1960).

[39]W. R. Busing and H. A. Levy, J. Chem. Phys. 26, 563 (1957); F. Holuj and J. Wieczorek, Can. J. Phys. 55, 654 (1977).

[40]H. W. Gruenigen and H. Barnighausen, Z. Anorg. Allg. Chem. 368, 53 (1969).

[41]H. D. Lutz, R. Heider, and R. A. Becker, Spectrochim. Acta. 28A, 871 (1972).

[42]JANAF Thermochemical Tables, 2nd Ed., NSRDS-NBS37, Catalogue Number C13.48:37 (U. S. Government Printing Office, Washington, D.C. 1971); JANAF Thermochemical Tables, J. Phys. Chem. Ref. Data 3, 311 (1974); 4, 1 (1975); 7, 793 (1978).

[43]D. D. Wagman, W. H. Evans, V. B. Parker, I. Halow, S. M. Bailey, and R. H. Schumm, Tech. Note U. S. Natl. Bureau Stand. 270-3 (1968); V. B. Parker, D. D. Wagman, and W. H. Evans, Tech. Note Natl. Bureau Stand. 270-6, (1971).

[44]*Handbook of Chemistry and Physics,* 60th ed., edited by R. C. Weast (CRC, Boca Raton, 1979).